

1 **Article**

2 **Discoveries**

3

4 **Title**

5 **Deciphering the wisent demographic and adaptive histories from individual**  
6 **whole-genome sequences**

7

8 **Authors and Affiliations**

9 Mathieu GAUTIER<sup>1,2§</sup>, Katayoun MOAZAMI-GOUDARZI<sup>3</sup>, Hubert LEVEZIEL<sup>4</sup>, Hugues  
10 PARINELLO<sup>5</sup>, Cécile GROHS<sup>3</sup>, Stéphanie RIALLE<sup>5</sup>, Rafał KOWALCZYK<sup>6</sup>, Laurence  
11 FLORI<sup>3,7§</sup>

12 <sup>1</sup> CBGP, INRA, CIRAD, IRD, Supagro, 34988 Montferrier-sur-Lez, France

13 <sup>2</sup> IBC, Institut de Biologie Computationnelle, 34095 Montpellier, France

14 <sup>3</sup> GABI, INRA, AgroParisTech, Université Paris-Saclay, 78350 Jouy-en-Josas, France

15 <sup>4</sup> UGMA, INRA, Université de Limoges, 87060 Limoges, France

16 <sup>5</sup> MGX-Montpellier GenomiX, c/o Institut de Génomique Fonctionnelle, Montpellier, France

17 <sup>6</sup> Mammal Research Institute, Polish Academy of Sciences, 17-230 Białowieża, Poland

18 <sup>7</sup> INTERTRYP, CIRAD, IRD, 34398 Montpellier, France

19

20 <sup>§</sup>Corresponding authors

21 Emails:

22 [mathieu.gautier@supagro.inra.fr](mailto:mathieu.gautier@supagro.inra.fr)

23 [laurence.flori@jouy.inra.fr](mailto:laurence.flori@jouy.inra.fr)

24

25 **Abstract**

26 As the largest European herbivore, the wisent (*Bison bonasus*) is emblematic of the continent  
27 wildlife but has unclear origins. Here, we infer its demographic and adaptive histories from  
28 two individual whole genome sequences via a detailed comparative analysis with bovine  
29 genomes. We estimate that the wisent and bovine species diverged from  $1.7 \times 10^6$  to 850,000  
30 YBP through a speciation process involving an extended period of limited gene flow. Our  
31 data further support the occurrence of more recent secondary contacts, posterior to the *Bos*  
32 *taurus* and *Bos indicus* divergence (*ca.* 150,000 YBP), between the wisent and (European)  
33 taurine cattle lineages. Although the wisent and bovine population sizes experienced a similar  
34 sharp decline since the Last Glacial Maximum, we find that the wisent demography remained  
35 more fluctuating during the Pleistocene. This is in agreement with a scenario in which wisents  
36 responded to successive glaciations by habitat fragmentation rather than southward and  
37 eastward migration as for the bovine ancestors.

38 We finally detect 423 genes under positive selection between the wisent and bovine lineages,  
39 which shed a new light on the genome response to different living conditions (temperature,  
40 available food resource and pathogen exposure) and on the key gene functions altered by the  
41 domestication process.

42

## 43 **Introduction**

44 The European bison, *Bison bonasus* (BBO), also known as the wisent, is an emblematic  
45 species of the European wildlife. The oldest fossil remains were found in Eastern Europe and  
46 trace back to the Late Pleistocene, approximately 12,000 Years Before Present (YBP)  
47 (Benecke 2005). The wisent is closely related to the North American bison (*Bison bison*),  
48 both species assumed to be derived from the extinct long-horned steppe bison (*Bison priscus*)  
49 which was widespread across the Northern hemisphere in the mid and upper Pleistocene (i.e.,  
50 781,000 to 11,700 YBP). However, several morphological and behavioral traits distinguish  
51 the wisent from its American relative. In particular, adults have generally a smaller body  
52 length (Kraśnińska and Kraśniński 2002), display a less hairy body and tend to be mixed feeders  
53 that combine browsing and grazing (Kowalczyk, et al. 2011; Merceron, et al. 2014) while  
54 American bison are essentially grazer. These various characteristics might be viewed as  
55 adaptation to living constraints associated to forest habitat that has been considered as a  
56 refuge (Kerley, et al. 2012; Bocherens, et al. 2015). During the mid and late Holocene, the  
57 wisent was distributed in central and eastern Europe with a longest survival in north-eastern  
58 Europe (Benecke 2005). Nevertheless, the progressive replacement of the open steppe by  
59 forest cover in early Holocene and the human population growth associated with the spread of  
60 farming during the middle Holocene lead to a reduction of its habitat (Kuemmerle, et al. 2012;  
61 Bocherens, et al. 2015). Hence, by the Middle Age, the wisent was only present in a few  
62 natural forests of North-Eastern Europe and finally faced extinction in the wild at the  
63 beginning of the 20<sup>th</sup> century (Pucek 2004). A species restoration program relying on a few  
64 tens of specimens kept in European zoos and private breeding centers was early initiated in  
65 the 1920's (Pucek 2004; Tokarska, et al. 2011). Thanks to these efforts, the wisent world  
66 population now consists of over 5,000 animals (including about 3,500 free-living individuals)  
67 that are mostly maintained in forests of eastern Europe (Kerley, et al. 2012; Raczyński 2015).  
68 The wisent is among the few large mammalian terrestrial species that survived the massive  
69 megafauna extinction of the last glacial/interglacial transition period, ca. 25,000-10,000 YBP  
70 (Lister and A.J. 2008; Lorenzen, et al. 2011). Characterizing the specific conditions of its  
71 survival may thus help understanding how organisms evolve in response to environmental  
72 change. In this study, we explore the wisent demographic and adaptive histories using  
73 individual whole-genome sequences from two males of the wisent lowland line (Tokarska, et  
74 al. 2011) living in the Białowieża Forest. To that end, we perform a detailed comparative  
75 analysis of these newly generated wisent genome sequences with individual genome

76 sequences representative of different European cattle breeds. Domestic cattle, the wild  
77 ancestor of which, the aurochs (*Bos primigenius*) went extinct in the 17<sup>th</sup> century, is indeed  
78 among the closest wisent relatives (Verkaar, et al. 2004) and benefits from abundant genomic  
79 resources (Liu, et al. 2009). Our genome-wide comparison provides an accurate  
80 characterization of the divergence between the bovine and wisent lineages and an estimation  
81 of their population size histories during Pleistocene and Holocene. In addition, the  
82 identification and functional annotation of genes under positive selection between both  
83 lineages shed light into the biological functions and the key adaptive traits that were affected  
84 by environmental constraints.

85

## 86 **Results and discussion**

### 87 *Comparison of wisent and cattle genomes reveals low amount of nucleotide* 88 *divergence.*

89 High-throughput sequencing data from two wisent bulls, namely BBO\_3569 and BBO\_3574,  
90 were each aligned onto the UMD3.1 cattle (BTA) genome assembly (Liu, et al. 2009). The  
91 read mapping statistics showed overall good performances (Table S1) with noticeably 97.4%  
92 (respectively 96.6%) of the reads being properly paired for the BBO\_3569 (respectively  
93 BBO\_3574). Conversely, following the same read mapping procedure but considering as a  
94 reference the *OviAr3* genome assembly (Jiang, et al. 2014) from the more distantly related  
95 domestic sheep (OAR) strongly altered the statistics (Table S1). Altogether, these mapping  
96 results provided support to consider the cattle genome as closely related enough to provide a  
97 good reference to assemble our wisent reads. For autosomes, an approximately 10X-coverage  
98 was achieved for both individuals (9.81X and 11.6X for BBO\_3569 and BBO\_3574  
99 respectively) with more than 95% of the (bovine) reference sequence covered by at least one  
100 read (Table 1). As expected for males, the bovine chromosome X was only slightly more than  
101 half covered (ca. 56.8% and 55.8% of the autosome coverage for BBO\_3569 and BBO\_3574  
102 respectively) due to the inclusion of pseudo-autosomal regions (PAR) in the estimation.  
103 Conversely, the (bovine) mitochondrial genome was found highly covered (>300X) for both  
104 individuals.

105 Interestingly, the estimated autosomal nucleotide divergence between the bovine genome and  
106 each wisent individual genome was found equal to 0.870% for BBO\_3569 and 0.882% for  
107 BBO\_3574 (Table 1) supporting a low amount of genome divergence between the two  
108 species. The estimated nucleotide divergence was about 1.37 times smaller for the

109 chromosome X than for autosomes, as already observed in the Chimpanzee vs. Human  
110 genome sequence comparison (Mikkelsen, et al. 2005). This is likely related to a higher  
111 mutation rate in the male compared to the female germ line in mammalian species (Li, et al.  
112 2002; Mikkelsen, et al. 2005). Also, the nucleotide divergence increased in distal  
113 chromosomal regions in both autosomes and X-chromosome comparisons while read  
114 coverage remained mostly uniform (Figure S1). Such a regional pattern, also reported in the  
115 aforementioned Chimpanzee vs. Human genome sequence comparison (Mikkelsen, et al.  
116 2005), might similarly result from the physical properties of the corresponding distal regions  
117 (i.e. high local recombination rate, high gene density and higher GC content). Indirectly,  
118 observing such a pattern for wisent sequences mapped onto the cattle genome assembly  
119 supports a low amount of chromosome rearrangements between the two species. Finally, the  
120 estimated nucleotide divergence for the mitochondrial genomes were about 4 times higher  
121 than for autosomes. This suggests an absence of recent maternal bovine introgression at least  
122 within the lineages of the two wisents we considered.

123

124 ***The wisent demography has been more fluctuating than the bovine one during***  
125 ***the whole Pleistocene.***

126 We further sought to characterize the genetic variability of the wisent population that has long  
127 been considered as a threatened species and is still classified as “vulnerable” by the  
128 International Union for Conservation of Nature (IUCN) red list (<http://www.iucnredlist.org/>).  
129 The estimated average (autosomal) heterozygosities, as approximated by the population  
130 mutation rate ( $\theta = 4N_e\mu_g$  where  $\mu_g$  represents the mutation rate per site and per generation  
131 and  $N_e$  the effective population size) measured on whole individual genomes, were consistent  
132 when considering either the BBO\_3569 ( $\hat{\theta} = 1.37 \times 10^{-3}$ ) or the BBO\_3574 ( $\hat{\theta} = 1.45 \times$   
133  $10^{-3}$ ) individual. Interestingly, both estimates were similar to the ones obtained on four  
134 individual cattle genomes representative of the Angus (AAN\_0037), Jersey (JER\_0009),  
135 Holstein (HOL\_0101) and Simmental (SIM\_0043) European cattle breeds which ranged from  
136  $\hat{\theta} = 1.27 \times 10^{-3}$  to  $\hat{\theta} = 1.97 \times 10^{-3}$  (Figure S2 and Table S2). The small heterozygosity  
137 observed for wisent might be explained by the sharp decline of its effective population size  
138 during the last 20,000 years (see below), but also by its more recent history since wisent  
139 experienced a strong bottleneck at the end of the First World War (Wójcik, et al. 2009;  
140 Tokarska, et al. 2011). However, we noted that our wisent estimates remained within the  
141 range observed for the four different European cattle breeds. This suggests that the

142 constitution of the Białowieża wisent herd from a small number of presumably poorly related  
143 founders and subsequent management (Pucek 2004) allowed to recover a reasonable amount  
144 of variability for the current population.

145 More generally, the patterns of variability observed at a local individual genome scale are  
146 informative about the demographic history of the population (Li and Durbin 2011). From our  
147 two individual genomes, we estimated the wisent past  $N_e$  using the Pairwise Sequentially  
148 Markovian Coalescent model (PSMC) introduced by Li and Durbin (2011), and compare it to  
149 that estimated for the bovine species based on each of the four cattle individual genomes  
150 aforementioned. Estimates of the scaled effective population sizes (in units of  $4N_e\mu_g$ )  
151 backward in time measured in scaled units of  $2\mu_y T$  (where  $T$  is in YBP, and  $\mu_y$  represents the  
152 mutation rate per site and per year) are plotted in Figure S3 for each of the six individual  
153 genome analyses (see Figure S4 for bootstrap confidence intervals of each history). Overall, a  
154 similar trend was observed within each species, irrespective of the individual considered  
155 (although the AAN\_0037 profile was more dissimilar than the three other cattle ones probably  
156 as a result of an overall lower coverage for this individual). By contrast, marked differences  
157 were found when comparing the inferred wisent and bovine population size histories. In  
158 particular, from backward time (in scaled units)  $t=10^{-3}$  to  $t=5.10^{-5}$  (Figure S3), wisent  
159 displayed more pronounced oscillations and from twice to three times higher effective  
160 population sizes. Because the PSMC model relies on local density of heterozygotes, using  
161 the bovine genome assembly as a reference to derive the analyzed individual wisent genomes  
162 (see Material and Methods) could have lead to some inferential biases (Nevado, et al. 2014).  
163 Nevertheless, the inferred wisent population size histories remained similar when considering  
164 a BBO consensus genome as a reference to derive the individual genome sequences (Figure  
165 S5). Similarly, given the close relatedness of the bovine and bison species, chromosomal  
166 rearrangements might remain negligible and should not have substantial effect on the overall  
167 inferred histories.

168 To facilitate biological interpretation of the observed demographic signals, we transformed  
169 the population size history profiles assuming  $\mu_y = 2.10 \times 10^{-9}$  (Liu, et al. 2006) to translate  
170 the time scale in YBP. Further, to translate the effective population sizes ( $N_e$ ) in real units, we  
171 assumed a generation time of  $g=6$  years (Keightley and Eyre-Walker 2000; Gautier, et al.  
172 2007), leading to  $\mu_g = g \times \mu_y = 1.26 \times 10^{-8}$ . The resulting backward in time estimates of  $N_e$   
173 are plotted in Figure 1. For both the wisent and bovine species, a sharp decline in  $N_e$  started at  
174 the end of the last glacial period, predating cattle domestication approximately 10,000 YBP as

175 already suggested for the latter species by MacLeod *et al.* (2013). This most presumably  
176 originates from a growing impact of human activities via hunting intensification and land  
177 anthropization especially after the development of agriculture (Soares, et al. 2010).  
178 Interestingly, the estimated wisent population sizes clearly oscillated according to the  
179 succession of glacial Pleistocene periods to *ca.* 500,000 YBP (viewed backward in time) with  
180 interglacial periods coinciding with lower population sizes. Conversely, from the Last Glacial  
181 Maximum (LGM) approximately 20,000 YBP (Clark, et al. 2009) to 150,000 YBP, the  
182 estimated bovine population sizes only slightly decreased, remaining always between 10,000  
183 to 20,000 individuals (more than two to three times lower than wisents, as mentioned above).  
184 Hence, even if the fluctuating pattern observed for wisent might correspond to actual changes  
185 in the population sizes, the comparison with the bovine species might lead to an alternative  
186 scenario of population fragmentation. In such a scenario, the alternation of population  
187 isolation events due to fragmentation of the habitats during glacial periods leads to an increase  
188 of the overall estimated  $N_e$  while a more continuously interbreeding between populations  
189 during interglacial periods leads to a decrease in the overall estimated  $N_e$ . Indeed, as recently  
190 evidenced by Mazet *et al.* (2015) when considering structured populations, changes in the  
191 gene flow patterns result in changes in the estimated  $N_e$  (even if the actual  $N_e$  remained  
192 constant) as PSMC assumes a panmictic model. As a result, one might expect an increase  
193 (respectively a decrease) in the estimated  $N_e$  when gene flow and thus the amount of  
194 connectivity between (sub)populations decreases (respectively increases). It is not possible  
195 from the PSMC analyses to distinguish between a scenario involving habitat fragmentation  
196 and a scenario of actual population size changes. However, it is tempting to speculate from  
197 the divergent patterns in the inferred population size across the wisent and bovine species that  
198 the ancient aurochs distribution range, possibly restrained to southern regions with more  
199 stable habitats, has only been partially overlapping the wisent one (hence the lower  $N_e$ ). In  
200 agreement with the “refugium theory” (Hofreiter and Stewart 2009), both species might have  
201 followed different strategies to survive during Pleistocene glaciations, the wisent remaining in  
202 small disconnected refugia while the aurochs migrated southward and possibly eastward  
203 (Mona, et al. 2010). Conversely, during interglacial periods, wisent may have retrieved a  
204 larger distribution area with a reconnection of isolated populations while the aurochs may  
205 have recolonized northern and central areas. Accordingly, the divergence of the wisent and  
206 the American bison which took place *ca.* 230,000 YBP (Hassanin, et al. 2013), might result  
207 from an absence of reconnection between populations separated in Eurasian and North-  
208 American refugia. Note also that the most recent common ancestor of all the Beringian bison

209 lived from 164,000 to 111,000 YBP (Shapiro, et al. 2004), a period that lies within the second  
210 peak observed in our estimated wisent population size history (Figure 1).

211 Finally, in agreement with MacLeod et al. (2013) that used a different inference model (and a  
212 different time calibration procedure), we also observed a steep increase (viewed backward in  
213 time) starting ca. 150,000 YBP in the inferred bovine population sizes that might actually be  
214 explained by the divergence of the taurine (BTA) and zebu (BIN) lineages (see e.g., Figure S5  
215 in Li and Durbin, 2011). Indeed, this divergence event is dated between 117,000 and 275,000  
216 YBP based on diversity of cattle mitochondrial sequences (Bradley, et al. 1996) and at  
217 147,000 YBP (with a 95% Highest Posterior Density interval ranging from 84,000 to 219,000  
218 YBP) using modern and radiocarbon-dated ancient mitochondrial DNA (Ho, et al. 2008). A  
219 similar increase starting about 1 MYA could also be observed for the ancestral wisent  
220 population size which coincides with the timing of BTA/BBO speciation (see below).

221

### 222 ***The wisent and bovine species diverged in the early Pleistocene and*** 223 ***experienced more recent secondary contacts***

224 To characterize the divergence between the BBO and BTA lineages, we further relied on the  
225 coalescent Hidden Markov Models (CoalHMM) framework (Hobolth, et al. 2007). Two  
226 models were considered corresponding to *i*) an isolation (I) model which assumes that the  
227 ancestral population split into two populations at time  $\tau_D$  into the past (Mailund, et al. 2011);  
228 and *ii*) an isolation-with-migration (IM) model which assumes that the ancestral population  
229 started to split into two populations at time  $\tau_2 = \tau_I + \tau_M$  and that these two populations exchanged  
230 gene with a migration rate  $M$  during a period  $\tau_M$  until a later time  $\tau_I$  when gene flow stopped  
231 (Mailund, et al. 2012). Under the I-model and assuming as above  $\mu_y = 2.10 \times 10^{-9}$ , the  
232 median estimate of  $\tau_D$  (over 10 Mbp segments) was found equal to  $1.20 \times 10^6$  YBP (ranging  
233 from  $1.02 \times 10^6$  to  $1.36 \times 10^6$ ) and  $1.23 \times 10^6$  YBP (ranging from  $1.01 \times 10^6$  to  $1.51 \times 10^6$ )  
234 when considering the alignments onto the UMD 3.1 bovine genome assembly of the  
235 BBO\_3569 and BBO\_3574 whole genome sequences respectively (Figure 2A). As expected,  
236 the  $\tau_D$  estimates were always intermediate between the estimated start ( $\tau_2$ ) and end ( $\tau_I$ ) times  
237 of the divergence period obtained under the IM-model (Figure 2B). Hence, when considering  
238 the BBO\_3569 (respectively BBO\_3574) sequence the median estimates of  $\tau_I$  and  $\tau_2$  allowed  
239 to define a period ranging from  $0.846 \times 10^6$  YBP to  $1.70 \times 10^6$  YBP (respectively from  
240  $0.864 \times 10^6$  YBP to  $1.72 \times 10^6$  YBP) for the divergence of the BBO and BTA lineages.  
241 During the corresponding divergence periods, the estimated number of migrants (per

242 generation) was found limited with median values of 0.56 and 0.61 for the BBO\_3569 and  
243 BBO\_3574 analyses respectively (Figure 2C). It should also be noticed that the ancestral  
244 population sizes estimated under both the I-model (median values of 62,120 and 65,740 for  
245 the BBO\_3569 and BBO\_3574 analyses respectively) and the IM-model (median values of  
246 50,750 and 53,430 for the BBO\_3569 and BBO\_3574 analyses respectively) were in  
247 agreement with those obtained above with the PSMC for the corresponding time period  
248 (Figure 1). Finally, as shown in Figure 2D, the comparison of the I- and IM-models of  
249 speciation provided a clear support in favor of the IM-model. From these CoalHMM analyses,  
250 we thus conclude that the BBO and BTA lineages diverged in the early Pleistocene (from  
251  $1.7 \times 10^6$  to 850,000 YBP), in agreement with previous studies that relied on alternative time  
252 calibrations (Bradley, et al. 1996; Troy, et al. 2001). Moreover, the divergence between these  
253 two lineages involved an extended period of limited gene flow similar to the speciation  
254 process previously reported in great apes (Mailund, et al. 2012).

255 However, both the I- and IM models were not designed to capture signals from more recent  
256 gene flow events associated to secondary contacts between the bovine and wisent species. To  
257 that end, we compared the relative abundance of ABBA and BABA site patterns (Green, et al.  
258 2010; Durand, et al. 2011) defined across the following four taxons: *i*) BBO, *ii*) BTA, *iii*) *Bos*  
259 *indicus* (BIN), and *iv*) OAR. Assuming a (((BTA;BIN);BBO);OAR) phylogeny (e.g.,  
260 (Buntjer, et al. 2002; Ho, et al. 2008; Jiang, et al. 2014)), ABBA (respectively BABA) sites  
261 are those at which the derived allele (“B”) is shared between the nonsister BIN and BBO  
262 (respectively BTA and BBO) lineages whereas BTA (respectively BIN) carries the ancestral  
263 allele (“A”), as defined by the OAR outgroup. In the absence of (recent) gene flow, both  
264 patterns may only result from incomplete lineage sorting and should be equally abundant in  
265 the genome while gene flow events between the BTA and BBO lineages would lead to a  
266 significant excess of BABA over ABBA sites (Durand, et al. 2011). Whether considering the  
267 BBO\_3569 or the BBO\_3574 sequencing data to define the BBO reference (see Material and  
268 Methods), we found a slight but significant excess of “BABA” (n=49,337 and n=58,032 for  
269 BBO\_3569 and BBO\_3574 respectively) over “ABBA” (n=48,004 and n=56,357 for  
270 BBO\_3569 and BBO\_3574 respectively). Accordingly, the *D-statistic* defined as the  
271 normalized difference in the counts of ABBA and BABA sites (Green, et al. 2010; Durand, et  
272 al. 2011) was found significantly negative for both the BBO\_3569 and BBO\_3574 derived  
273 consensus sequences with values equal to -1.25% (s.d.=0.032% ; Z=39.0) and -1.37%  
274 (s.d.=0.031% ; Z=44.4) respectively. The corresponding proportion of BBO ancestry into  
275 (European) cattle was found equal to  $\hat{f} = 0.143\%$  (s.d.=0.004%) which is actually a

276 conservative minimum (Green, et al. 2010). Assuming a constant population size, the bias is  
277 equal to  $t_a/t_s=0.28/0.85=0.33$  in the worst scenario since  $t_a$  represents the timing of the BBO  
278 and BTA admixture (<275,000 YBP, the lower bound of the estimated divergence between  
279 the taurine and zebu lineages, see above) and  $t_s$  the timing of the bovine/wisent speciation  
280 (>850,000 YBP, the upper bound found above under the IM-model). Even if the resulting  
281 corrected proportion ( $\widehat{f}^* \approx 0.4\%$ ) remains very small, the observed (significant) footprints of  
282 BBO ancestry into the genomes of European cattle supports the occurrence of secondary  
283 contacts between these two lineages that are posterior to the *Bos taurus* and *Bos indicus*  
284 divergence (ca. 150,000 YBP, see above). Analyzing non-European (e.g., African) taurine  
285 genomes might allow to refine the timing of such secondary contacts by assessing whether or  
286 not they still occurred after (taurine) cattle domestication (ca., 10,000 YBP). To that respect  
287 also, sequencing individuals (or fossil remains) from extant (*Bison bison*, most particularly) or  
288 extinct (e.g., *aurochs* and *Bison priscus*) sister species would also be very informative.  
289 Conversely, it should be noticed that genomic data from *Bison* species would also allow to  
290 quantify the proportion of bovine ancestry (if any) in the BBO genome.

291

### 292 ***Identification and functional annotation of genes under positive selection***

293 To identify genes under positive selection between the wisent and bovine lineages, we  
294 computed the  $Ka/Ks$  ratio of nonsynonymous ( $Ka$ ) and synonymous ( $Ks$ ) substitution rates  
295 (Kimura 1983) for 17,073 protein sequence alignments between the BBO and BTA genomes.  
296 As expected from the effect of purifying selection (Hurst 2002), the average  $Ka/Ks$  was found  
297 equal to 0.273 (ranging from 0.00 to 17.2) with a distribution highly shifted towards 0 (Figure  
298 S6). Transcripts with  $Ka/Ks>1$  were further considered under positive selection leading to the  
299 annotation of 425 genes ready to functional and gene network analyses (see Material and  
300 Methods, Table S3). Overall, the most significant functions underlying these genes are related  
301 to i) nervous system; ii) immune and inflammatory responses; iii) embryonic and organ  
302 development; iv) cellular morphology and organization and; v) skeletal and muscular  
303 disorders (Table S4). Figure 3 illustrates the connection of the selected genes that were  
304 annotated with their key underlying functions and Table 2 gives a more detailed list of  
305 functions and sub-functions. Interestingly, many genes are related to several functions (Table  
306 S5), suggesting a pleiotropic role and more strikingly, 85% of the genes participated to a  
307 global gene network which is defined by six significant networks connected by up to 11  
308 common molecules (Table S6 and Figure S7). Note that very similar results are obtained

309 when restricting the functional analysis to the 359 selected genes that are one to one orthologs  
310 between cattle and sheep (see Table 2 and Table S4). Thanks to the method we used to define  
311 BBO/BTA gene sequence alignments, this suggests that our annotation remains somewhat  
312 robust to extra variation that could have been identified when mapping BBO reads in genic  
313 regions belonging to large gene families or due to Copy Number Variants in the sequenced  
314 BBO individuals.

315 Among the genes under selection, some underlie obvious distinctive features between wisent  
316 and cattle providing in turn insights into the wisent adaptive history (Table 2, Figure 3 and  
317 Table S6). First, KRT74 and DCS3 that are involved in woolly hair development and  
318 hypotrichosis, respectively (Ayub, et al. 2009; Shimomura, et al. 2010) and GPR50 that plays  
319 a role in thermogenesis (Bechtold, et al. 2012) might be directly related to wisent adaptation  
320 to colder climatic conditions (Table 2, Table S4). Second, genes encoding olfactory and taste  
321 receptors are probably footprints of feeding behavior modifications, resulting *e.g.*, from food  
322 resource differences in forest *versus* steppe habitat (trees-shrubs *versus* grass). Third, the  
323 many genes related to immune and inflammatory responses (through their key role in  
324 activation, migration, binding, expansion and modulation of a broad range of immune cells,  
325 Table S5) may sign adaptation of wisent and bovine to different pathogen exposures. Fourth,  
326 several genes were found involved in lipid metabolism or mammary gland development  
327 (Table S5), likely the result of selection in cattle for improved milk production performances.  
328 More strikingly, the functional analysis of the genes under selection highlighted physiological  
329 functions associated to the domestication process (Figure 3, Table 2, Table S6), as expected  
330 from the close relatedness of wisent and domestic cattle. These functions underlie both key  
331 processes of nervous system (*e.g.*, neurogenesis, neurulation, remodeling of dendrites,  
332 differentiation of some neural cells) and by-product phenotypes of domestication (*e.g.*,  
333 skeletal and muscular disorders, hair and skin properties, vision, hearing, reproduction). Our  
334 analysis thus gives an empirical support to the unified explanation of the “domestication  
335 syndrome” in mammals (*i.e.*, the general combination of observed traits in domestic  
336 mammals) formulated by Wilkins and collaborators (Wilkins, et al. 2014) following the  
337 pioneering work by D.K. Belyaev and L. Trut (Belyaev 1979; Trut, et al. 2009). This  
338 explanation accords a central role to the neural crest through its developmental reduction as a  
339 result of the primary domestication pressure (*i.e.*, the taming of animals). Furthermore,  
340 because neural crest cells are also cellular precursors of many different cells (*e.g.*, osteocytes,  
341 chondrocytes, odontocytes and melanocytes), this reduction indirectly produces various  
342 secondary phenotypic changes (*e.g.*, skeletal and craniofacial morphological modifications or

343 coat-colour changes). For instance, such an indirect relationship is well supported by studies  
344 on coat coloration in wild and domesticated animals (Cieslak, et al. 2011) and the description  
345 coat-colour associated mutations with pleiotropic effects (Reissmann and Ludwig 2013).  
346 Also, the numerous genes detected under selection and involved in immune response (Table 2  
347 and Figure 3) might be indirectly related to the domestication process. During this process and  
348 afterwards, herding conditions may have incidentally lead to an increased pathogen exposure  
349 of domestic cattle due to proximity with individuals from the same or different species  
350 (Freeman, et al. 2008).

351

## 352 **Conclusions**

353 To characterize the wisent demographic and adaptive histories, we carried out whole genome  
354 sequencing of two males from the Białowieża lowland line. Although still considered as a  
355 vulnerable species, our results show that the conservation plan and subsequent management  
356 practices have been efficient to recover a reasonable amount of genetic variability that now  
357 compares to that observed in commercial cattle breeds. We further confirmed at the  
358 nucleotide level, the close relatedness of the wisent and cattle species without any evidence  
359 for recent gene flow (i.e., during historical times) between these two species. We estimated  
360 that the divergence between the bovine and wisent lineages occurred in the early Pleistocene  
361 through a speciation process involving limited gene flow, lasting from  $1.7 \times 10^6$  to 850,000  
362 YBP. We also found evidence for more recent secondary contacts, posterior to the *Bos taurus*  
363 and *Bos indicus* divergence (ca. 150,000 YBP), between the wisent and (European) taurine  
364 cattle lineages. Interestingly, whole individual genome based demographic inference  
365 highlighted contrasting patterns in both species that might be reminiscent of different adaptive  
366 strategies (habitat fragmentation versus migration) to survive Pleistocene glaciations. Our  
367 results are indeed in agreement with a scenario in which wisent survive in refugee pockets  
368 during glaciations (leading to habitat fragmentation) while aurochs migrate southward (and  
369 possibly eastward) where climate remained more temperate (Sommer and Nadachowski  
370 2006). It is tempting to speculate that these two alternative strategies might have contributed  
371 to the survival of both species to the large mammals Quaternary extinction. Our results also  
372 show that wisent and aurochs display a similar trend towards extinction from the Last Glacial  
373 Maximum, 20,000 years ago that is concomitant to human population growth (spread of  
374 farming and increased hunting pressure), to climate warming and to vegetation changes (e.g.,  
375 replacement of open-steppe by forests). For the wisent, in particular, the Holocene period was

376 characterized by a tendency to shift towards forested habitats imposing a significant diet  
377 change (Kerley, et al. 2012; Bocherens, et al. 2015). These new constraints left footprints at  
378 the genomic level as illustrated by the genes that we found under selection when comparing  
379 the wisent and bovine lineages, i.e., genes involved in feeding behavior and in adaptation to  
380 temperature conditions and to pathogen exposure. Conversely, wisent being the closest extant  
381 wild relative species of domestic cattle, several of the genes under selection could be related  
382 to the adaptive response to cattle domestication via their implication in nervous system  
383 development and in the expression of by-product domestication phenotypes. Strikingly, this  
384 result is in line with unified explanation of the domestication syndrome in mammals  
385 formulated by Wilkins *et al.* (2014) giving a shared developmental connection of these  
386 diverse traits via neural crest cells.

387

## 388 **Materials and Methods**

### 389 ***Sample origin.***

390 Genomic DNA of two male wisents, namely BBO\_3569 and BBO\_3574, was extracted from  
391 blood samples collected in 1991 in the Białowieża forest. More precisely, BBO\_3569 and  
392 BBO\_3574 belong to the genetically isolated pure lowland line which originates from seven  
393 founders kept in zoo and private breeding centers and used for the species restoration program  
394 at the beginning of the 1920's (Tokarska, et al. 2009). In 1952, 40 of their descendants that  
395 were born in captivity were re-introduced to the wild in the Polish part of the Białowieża  
396 forest, the so-called lowland line now including more than 2,000 individuals (i.e., about half  
397 of the world wisent population).

### 398 ***High-throughput sequencing of two wisents.***

399 The Illumina TruSeq DNA sample preparation kit (FC-121-2001, Illumina Inc., San  
400 Diego, USA) was used according to the manufacturer's protocol. Libraries were then validated  
401 on a DNA1000 chip on a Bioanalyzer (Agilent) to determine size and quantified by qPCR  
402 using the Kapa library quantification kit (KAPA) to determine concentration.

403 The cluster generation process was performed on cBot (Illumina Inc.) by using the Illumina  
404 Paired-End DNA sample preparation kit (FC-102-1001, Illumina Inc.). Both BBO individuals  
405 were further paired-end sequenced on the HiSeq 2000 (Illumina Inc.) using the SBS  
406 (Sequence By Synthesis) technique. Base calling was achieved by using the RTA software  
407 (Illumina Inc.). Reads of 100 bp from both sides of the fragments were thus obtained after this  
408 step. Quality control of the sequences was checked using the FastQC software.

#### 409 ***Mapping wisent sequencing reads onto the bovine genome.***

410 In total, 331,975,598 and 407,585,788 reads paired in sequencing were available for  
411 BBO\_3569 and BBO\_3574 respectively after Illumina Quality Check. After removal of  
412 sequencing adapters, these reads were mapped onto the UMD3.1 cattle (*Bos taurus*) reference  
413 genome assembly (Liu, et al. 2009) using default options of *aln* and *sampe* programs from the  
414 *bwa* (version 0.6.2) software package (Li and Durbin 2009). In total, 92.7% (respectively  
415 92.2%) of the reads from the BBO\_3569 (respectively BBO\_3574) library were successfully  
416 mapped onto the bovine assembly, 94.5% (respectively 93.6%) of which being properly  
417 paired. Read alignments with a mapping quality Phred-score MAPQ<20 and PCR duplicates  
418 were further removed using the *view* (option *-q 20*) and *rmdup* programs from the *samtools*  
419 (version 0.1.19) software package (Li and Durbin 2009). The resulting bam files are available  
420 for download from the Sequence Read Archive repository (<http://www.ncbi.nlm.nih.gov/sra>)  
421 under the accession number SRP070526. It should be noted that mapping the wisent reads  
422 onto the preliminary Y-chromosome sequence from the BosTau7 assembly (available at  
423 <http://www.genome.ucsc.edu/>) lead to a high proportion of reads improperly paired and only  
424 about 12% of the BTAY sequence was covered with an unexpected high read coverage  
425 (>60X). We thus decided not to consider the chromosome Y in further analyses.

#### 426 ***Construction of individual wisent consensus genome sequences.***

427 For the analyses of BBO/BTA cattle divergence, consensus genome sequences were built for  
428 each individual by first generating a *mpileup* file considering each European bison *bam*  
429 alignment file separately and using the *mpileup* program from the *samtools* (version 0.1.19)  
430 software package (Li and Durbin 2009) run with *-C 50* and *-d 5000* options. For each BBO  
431 individual and at each position (in the bovine reference assembly), the retained consensus  
432 base was randomly sampled among the aligned bases after discarding those showing a Base  
433 Alignment Quality BAQ>30 (allowing to account for uncertainty resulting from small indels).  
434 Such a procedure was aimed at limiting biases towards the bovine reference base at BBO  
435 heterozygous sites. Finally, positions with a read depth DP<3 and DP>30 (i.e., three times the  
436 average individual read coverage), or for which the retained base was supported by less than 2  
437 reads (to limit sequencing error biases) were treated as N (not called) in the consensus  
438 sequences.

#### 439 ***Whole genome sequence of four individual bovine genomes.***

440 Four bovine individual whole genome sequences were obtained from the 1000 bull genome  
441 projects data (Daetwyler, et al. 2014) stored in the NCBI *sra* archive website

442 (<http://www.ncbi.nlm.nih.gov/sra>). More precisely, the four males selected were AAN\_0037,  
443 HOL\_0101, JER\_0009 and SIM\_0043 and belonged to the Angus, the Holstein, the Jersey  
444 and the Simmental European taurine breeds respectively and were sequenced at a roughly  
445 similar coverage (8.2X, 9.6X, 11X and 10X respectively) than the European bisons. As for the  
446 European bison sequencing data, reads with a MAQ<20 and PCR-duplicates were filtered out  
447 from the downloaded *bam* files using the *view* (option *-q 20*) and the *rmdup* programs from  
448 the *samtools* (version 0.1.19) software package (Li and Durbin 2009).

449 ***Testing for recent gene flow events between the BBO and BTA lineages using***  
450 ***the ABBA-BABA statistics.***

451 To count the number of sites with ABBA and BABA patterns across the BTA, BIN, BBO and  
452 OAR lineages, we first identified sites displaying a “BA” pattern by comparing the consensus  
453 sequences derived from each individual BBO to the OAR reference genome assembly. To  
454 that end and following the same procedure and program options as the ones described above  
455 for the mapping of reads onto the UMD3.1 bovine genome assembly (see Results section and  
456 Table S1), we mapped the sequencing reads originating from the BBO\_3569 and BBO\_3574  
457 European bisons onto the *OviAr3* OAR genome assembly (Jiang, et al. 2014). Based on the  
458 resulting *mpileup* alignment files, we then defined for each BBO individual a consensus base  
459 as described above (section “Construction of individual consensus genome sequences”)   
460 except that the upper read depth threshold was set to 20 (to account for the lower coverage  
461 when mapping reads onto the ovine genome as summarized in see Table S1). The “BA” sites  
462 were those at which the consensus base differed from the OAR reference. To further identify  
463 whether the “A” or “B” allele was present in the BTA and BIN genomes, the OAR sequences  
464 surrounding each of these sites were extracted (60 nt upstream and 60 nt downstream) and  
465 aligned onto the BTA UMD3.1 (Liu, et al. 2009) and BIN genome (Canavez, et al. 2012)  
466 assemblies using the *blat* (version v35x1) software with default options except for the  
467 minimum sequence identity that was set to 95% (Kent 2002). For a given comparison,  
468 sequences aligning to more than 10 positions were discarded from further analyses (otherwise,  
469 the alignment displaying the highest score was retained). Similarly, sites for which a base  
470 different from the “A” and “B” alleles was present in the BIN or BTA sequence or the 2  
471 upstream and downstream flanking nucleotides did not perfectly match were although  
472 discarded. In total, 10,035,538 (respectively 11,533,956) “BA” sites could be called in both  
473 the BIN and BTA assemblies based on the BBO\_3564 (respectively BBO\_3574) genomic  
474 data. From the observed numbers of “ABBA” and “BABA”, we then computed the *D-*

475 *statistics* and both their associated standard error and their corresponding Z-score (to assess  
476 whether  $D$  significantly differs from zero) using a Weighted Block Jackknife with 5 Mb blocks  
477 (Green et al., 2010; Durand et al., 2011). To further estimate the proportion of BBO ancestry  
478 in the BTA genome, we relied on the estimator proposed by Durand et al. (2011) here defined  
479 as  $\hat{f} = \frac{S(ZEB,BTA,BBO\_3574,OAR)}{S(ZEB,BBO\_3574,BBO\_3569,OAR)}$ , where  $S(P1,P2,P3,P4)$  represents the difference of the  
480 “ABBA” and “BABA” sites numbers assuming a  $((P1;P2);P3);P4$  phylogeny and estimated  
481 following a procedure similar to the one described above. As for the  $D$ -*statistic* estimates, the  
482 standard deviation of  $\hat{f}$  was computed using a Weighted Block Jackknife with 5 Mb blocks.

### 483 ***Estimation of genetic heterozygosity from individual genomes.***

484 Genetic heterozygosities were estimated from the individual genome alignments onto the  
485 UMD 3.1 cattle assembly (i.e., based on the *mpileup* files described above) using *mlrho*  
486 version 2.8 (Haubold, et al. 2010). Note that *mlrho* actually implements a maximum  
487 likelihood estimator of the population mutation rate ( $\theta = 4N_e\mu_g$ ), which fairly approximates  
488 heterozygosity under an infinite sites model (and providing  $\theta$  is small), while simultaneously  
489 estimating sequencing error rates and accounting for binomial sampling of parental alleles  
490 (Lynch 2008). For a given individual genome alignment, only sites covered by 3 to 30 reads  
491 (after discarding bases with a  $BAQ < 25$ ) were retained in the computation (Table S2).

### 492 ***Population size history inference using the psmc.***

493 Effective population sizes in units of  $4N_e\mu_g$  were estimated backward in time (in units of  
494  $2\mu_y T$ ) based on individual whole genome sequences under the PSMC model using the  
495 program *psmc* (version 0.6.4) program (Li and Durbin 2011). Briefly, the analyzed individual  
496 whole genome sequences were obtained from the above described *mpileup* files (aligned onto  
497 the UMD3.1 cattle assembly) that were processed (individually) with *bcftools* (version 0.1.19)  
498 (Li and Durbin 2009) using the  $-c$  option. The resulting *vcf* files were further converted into  
499 *fastq* files using the *vcf2fq* utility of the *vcfutils.pl* program available in the *samtools* (version  
500 0.1.19) suite (Li and Durbin 2009) discarding sites located less than 5 nucleotides from an  
501 indel ( $-l 5$  option) and covered by less than 3 or more than 30 reads ( $-d 3 -D 30$  options). As  
502 originally described, the *psmc* program was finally run with default options except for the  
503 pattern of atomic time intervals ( $-p$  option) that were set to “4+25\*2+4+6” on a reduced  
504 version of the (autosomal) genomes (*psmcfa* files), with consecutive sites grouped into  
505 consecutive bins of 100 nucleotides marked as “K” (at least one heterozygote), “T” (no  
506 heterozygote sites) or “N” (less than 90 called sites).

507 ***Characterization of the divergence between BBO and BTA lineages under the***  
508 ***coalHMM framework.***

509 For each BBO individual consensus genome sequence, genome alignment onto the UMD 3.1  
510 bovine reference assembly (see the section “Construction of individual consensus genome  
511 sequences” above) was divided into 10 Mbp non overlapping segments. Segments mapping to  
512 the (bovine) X-chromosome or with more than 500,000 (5 %) missing information (i.e., an  
513 uncalled base in either the BTA or BBO sequence) were further discarded leading to a total of  
514 123 and 177 available segments for the BBO\_3569 and BBO\_3574 alignments respectively.  
515 Maximum likelihood inference was then carried out independently for each segment using the  
516 scripts *isolation-model.py* (version 1.1) for the I-model, and the *initial-migration-model.py*  
517 (version 1.2) for the IM-model, from the *IMCoalHMM* software package  
518 (<https://github.com/mailund/IMCoalHMM>). More precisely, the parameters underlying the I-  
519 model include the split time  $\tau_D$  (in units of  $\mu_y T$ ) and also the ancestral effective population  
520 size (in scaled units of  $\theta = 4N_e\mu_g$ ) and the recombination rate  $\rho$  (in scaled units of  $\mu_g$ ) that  
521 both parameterize the underlying coalescent process. The parameters underlying the IM-  
522 model include the times  $\tau_I$  (completion of the split) and the IM period length  $\tau_M$  that both are  
523 units of  $\mu_y T$ , the migration rate  $M$  (in number of migration per substitution) and  $\theta$  and  $\rho$  (as  
524 for the I-model). Note that the product  $M \times (\theta/2)$  corresponds to the estimated number of  
525 migrant per generation (in the usual units of  $2N_e m$  where  $m$  is the net migration rate) over the  
526 IM period. Finally, for model comparison purposes, the Akaike Information Criterion (AIC)  
527 was computed as  $AIC_I = 2x(3-l)$  for the I-model and  $AIC_{IM} = 2x(5-l)$  for the IM-model where  $l$   
528 represents the estimated log-likelihood of the corresponding model.

529 ***Detection of genes under selection.***

530 Based on the alignment of the BBO\_3569 and BBO\_3574 individual sequences onto the  
531 bovine UMD 3.1 reference genome assembly (*mpileup* file described above), a consensus  
532 BBO sequence was derived for all the  $n=22,091$  (bovine) ENSEMBL protein-coding  
533 sequences as defined in the UCSC genome database (<http://genome.ucsc.edu/>). At a given  
534 position, the retained consensus base corresponded to the most represented one among all the  
535 aligned reads from both the BBO\_3569 and BBO\_3574 individuals and after discarding bases  
536 with a  $BAQ < 30$ . Positions with a read depth  $DP < 3$  and  $DP > 60$  (three times the average  
537 coverage of BTA genome assembly by the combined BBO\_3569 and BBO\_3574 read  
538 sequencing data) were treated as N (not called) in the consensus sequences. BBO consensus  
539 protein sequences with more than 10% “N” were discarded from further analysis leading to a

540 total of n=19,372 remaining BBO/BTA alignments (with 1.11% “N” on average). For 1,306  
541 (6.74%) of these, no nucleotide differences could be observed between the obtained BBO  
542 consensus sequence and the BTA one. Nonsynonymous (Ka) and synonymous (Ks)  
543 substitution rates were then computed using *KaKs\_calculator v1.2* (Zhang, et al. 2006)  
544 assuming a MLWL model to estimate the number of synonymous and nonsynonymous sites  
545 (Zhang, et al. 2006) allowing the estimation of the *Ka/Ks* ratio for a total of 17,073 protein  
546 coding sequences.

### 547 ***Functional annotation of candidate genes under positive selection and gene*** 548 ***network analysis.***

549 Among the 17,073 Ensembl transcripts ID corresponding to the protein coding sequences for  
550 which a *KaKs* ratio was estimated, 873 transcripts with a *KaKs* ratio above one were  
551 considered under positive selection.

552 Functional annotation of these transcripts and networks analyses were carried out with the  
553 Ingenuity Pathway Analysis software (IPA, Ingenuity@Systems, [www.ingenuity.com](http://www.ingenuity.com)).  
554 Among the 873 transcripts with a *KaKs* ratio above one, 481 transcript ID were mapped to the  
555 Ingenuity Pathway Knowledge Base (IPKB) and were representative of 425 individual genes  
556 ready for analysis (Table S3). A total of 405 of these transcripts were further identified as one  
557 to one orthologs between cattle and sheep, using Ensembl orthology information  
558 (<http://www.ensembl.org/biomart/>). The top significant functions and diseases (p-value<0.05)  
559 were obtained by comparing functions associated with the 425 (among which 359 were one to  
560 one orthologs between cattle and sheep) genes against functions associated with all genes in  
561 our reference set (14,465 transcripts mapped in IPKB from the 17,073 transcripts ID that were  
562 analyzed) using the right-tailed Fisher's exact test. A total of 262 genes (among which 151  
563 were one to one orthologs between cattle and sheep) participated to the significant functions  
564 thus determined (Table S5).

565 Among the 425 genes, 367 genes (among which 324 were one to one orthologs between cattle  
566 and sheep) were included in network analyses. For each network that contains at most 140  
567 molecules, a score S was computed based on a right-tailed Fisher exact test for the  
568 overrepresentation of the genes with a *KaKs* ratio>1 ( $S=-\log(p\text{-value})$ ). A network was  
569 considered as significant when  $S>3$ .

570

571

### 572 **Acknowledgements and funding information**

573 The authors wish to thank Anna Madeyska-Lewandowska (Private Veterinary School,  
574 Warsaw, Poland) that provided the *Bison bonasus* samples in the early 1990's as part of a  
575 collaborative research project on the characterization of casein variants. We are also grateful  
576 to the four anonymous reviewers for their very helpful and constructive comments. This work  
577 was supported by an INRA (Institut National de La Recherche Agronomique)-Animal  
578 Genetics Department Grant (AFROSEQ project).

579 Sequencing data (bam files) are available for download from the Sequence Read Archive  
580 repository (<http://www.ncbi.nlm.nih.gov/sra>) under the accession number SRP070526.

581

582 **TABLES**

583

584 **Table 1: Read mapping statistics from the alignment of each BBO\_3569 and BBO\_3574**  
 585 **European bison genome sequences onto the UMD 3.1 cattle genome assembly (Liu, et al.**  
 586 **2009).**

587

Chromosome Type (BTA)	Size (in bp)	Coverage (% of sequence covered)*		Average nucleotide divergence in % (number of sites compared)**	
		BBO_3569	BBO_3574	BBO_3569	BBO_3574
Autosomes	2,512,082,506	9.81 (95.5)	11.6 (95.7)	0.870 (2.27x10 <sup>9</sup> )	0.882 (2.29x10 <sup>9</sup> )
X-chromosome (including PAR)	148,823,899	5.57 (90.9)	6.48 (91.2)	0.636 (1.11x10 <sup>8</sup> )	0.642 (1.17x10 <sup>8</sup> )
Mitochondria	16,338	397 (97.7)	302 (97.1)	3.58 (1.18x10 <sup>4</sup> )	3.41 (1.20x10 <sup>4</sup> )

588

589 \* For each individual, the average read coverages (after alignment) over autosomes, the X-chromosome and the  
 590 mitochondria are given together with the overall percentages of sites from the corresponding reference sequences  
 591 covered with at least one read.

592 \*\* For each type of chromosomes, the average nucleotide divergence between the cattle reference genome and  
 593 each European bison individual consensus sequence is given (see Material and Methods).

594

595

596 **Table 2: Main genes under selection listed by key functions and by presumed**  
 597 **adaptation.**

Key Function	Color in Figure 3	Sub-function	Genes	Presumed adaptation
Hair development	grey	Growth of hair follicles	CDKN2A	Adaptation to temperature conditions (cold/temperate)
		Wooly hair	KRT74*	
		Hypotrichosis	DSC3*	
Thermogenesis	grey		GPR50*	
Gustation	white		PKD2L1*, TAS1R1*, TAS2R16*, TAS2R46*	
Nervous system	purple	Olfaction	ADH7, CNGB1*, Olfr1178*, Olfr1179, Olfr1231*, Olfr1280, Olfr1353, Olfr1358*, Olfr1535, Olfr424*, Olfr49, Olfr541, Olfr600*, Olfr606, Olfr610*, Olfr711, Olfr867*, Olfr905, Olfr922*, Olfr963*, OR10AG1, OR10J5*, OR10V1*, OR12D3*, OR13F1, OR1E2*, OR1J1*, OR1M1*, OR2AG2*, OR2D2*, OR2M5, OR4C12, OR4C46*, OR4F15*, OR4F6, OR51A7*, OR52E8*, OR52H1, OR52R1, OR5C1, OR5M11*, OR6K2*, OR6N2*, OR6Y1*, OR7G3, OR8A1, OR9K2	Adaptation to available food resources and vegetation diversity (Forest/steppe habitat)
		Neurogenesis, neurulation	CD44*, CD9*, CDKN2A, GZMB*, NEIL3*, OR8A, SIX1*, SP4*, TTL8*, VASP*	Wildlife/Domestication
Hearing	blue		CLIC5*, FOXL1, SIX1*, SYNE4*	Wildlife/Domestication
Vision	blue		CNGB1*, GPNMB, LCA5*, MYOC*, OCA2*, TMEM5	Wildlife/Domestication
Pigmentation	blue		OCA2*	Wildlife/Domestication
Skeletal and muscular development	blue		CDKN2A, CKAP2L*, FAM111B*, FOXI1*, KLF5, NCOA1*, NDUFS6, PIGV*, PLG*, RNF135*, SLC17A3*, WISP3*	Wildlife/Domestication
Reproduction	orange		ACR, AGER*, CD44*, CD48, CD55*, CD9*, CDKN2A, FETUB*, FOXI1*, NCOA1*, PER2*, PLG*, SFTPC*, SPAM1*, ZP2*	Wildlife/Domestication
Immune and inflammatory responses	pink		ADAM8, AGER*, ANGPTL3*, APOBEC3B*, CCL16*, CCL24*, CCL5*, CD180*, CD1E*, CD244*, CD4*, CD44*, CD48, CD55*, CD72*, CD9*, CDKN2A, CFH, CKAP2L*, CXCL16*, EVI2A*, FCAR*, FCRL1*, FCRL3*, HBD*, HLA-B, HLA-DMB*, ICAM1*, IFI44*, IFNA16, IFNAR1*, KLRC1, KLRD1*, Klrk1*, LAG3*, MAVS*, OR12D3*, PGLYRP2*, PIGV*, PLG*, PPP1R15A*, PRSS16*, RHBDD3*, RTP4, SFTPD, SIRPA, SLC17A3*, SLC39A4*, SPN*, TF*, THPO*, TMPRSS11D*, TNFSF9*, TRIM40*, ULBP3, VASP*, XAF1*	Resistance/Tolerance to pathogens (linked to wildlife/domestication)
Metabolism	yellow	Lipid metabolism	ACADL*, ANGPTL3*, APOF*, BCO2*, CCL5*, CD4*, CD9*, CIDEC*, CYP4B1*, GHRL*, GPLD1*, HSD17B3*, MOGAT3, PLIN2*, RDH16*	Adaptation to diet Artificial selection on dairy traits
Embryonic and organ development	green	Mammary gland development	CD44*, CDKN2A PLG*,	Artificial selection on dairy traits
		Other	ACR, AGER*, CD44*, CD9*, CDKN2A, CKAP2L*, CLDN15*, FCAR*, FETUB*, FOXI1*, ICAM1*, IFNAR1*, KLF5, MAVS*, NCOA1*, ODC1, PLG*, POU2F1*, RNF135*, SFTPD, SIX1*, SPAM1*, TF*, THPO*, VASP*, VGLL1*, ZP2*	

598 \*One to one orthologs between cattle and sheep

## 599 **FIGURE LEGENDS**

600

### 601 **Figure 1. Population size histories inferred from the two wisent and the four bovine** 602 **genomes under the PSMC model.**

603 Backward in time (in YBP) estimates of the effective population sizes derived from the *psmc*  
604 analyses of the BBO\_3569 and BBO\_3574 individual wisent genomes and the AAN\_0037,  
605 HOL\_0101, JER\_0009 and SIM\_0043 bull bovine genomes and assuming  $\mu_y = 2.10 \times 10^{-9}$   
606 (Liu, et al. 2006) and  $g=6$  (Keightley and Eyre-Walker 2000; Gautier, et al. 2007). At the  
607 bottom of the figure, the timing of cattle domestication and the zebu (BIN) and taurine (BTA)  
608 divergence (Ho, et al. 2008) are indicated by a dark red triangle while the timing interval of  
609 the bovine and wisent divergence (see the main text) is indicated by dark red arrows.  
610 Similarly, European ice ages (Würm, Riss, Mindel and Günz glacial stages) according to the  
611 Penck and Bruckner work (Penck and Brückner 1901-1909) cited in (Elias 2013) are indicated  
612 by blue intervals at the top of the figure. Finally, the Last Glacial Maximum (LGM), ca.  
613 20,000 YBP (Clark, et al. 2009), is indicated by a vertical blue dotted line.

614

### 615 **Figure 2. Characterization of the divergence between the BBO and BTA lineages under** 616 **the isolation and the isolation-with-migration models.**

617 A. Estimation of the time  $\tau_D$  of divergence between the BBO and BTA lineages under the  
618 Isolation model (that assumes a clean split). The two violin plots show the distribution of  $\tau_D$   
619 estimates obtained for each 10 Mbp non-overlapping segments from the alignments of the  
620 BBO\_3569 (n=123 segments) and BBO\_3574 (n=177 segments) whole genome sequence  
621 onto the UMD 3.1 bovine genome assembly. Time scale was translated into YBP assuming  
622  $\mu_y = 2.10 \times 10^{-9}$  (Liu, et al. 2006).

623 B. Estimation of starting ( $\tau_2$ ) and ending ( $\tau_1$ ) time estimates of the divergence between the  
624 BBO and BTA lineages under the Isolation-with-Migration model (that assumes the two  
625 ancestral lineages exchange migrants between  $\tau_2$  and  $\tau_1$ ). The violin plots show the  
626 distribution of  $\tau_2$  and  $\tau_1$  time estimates obtained for each 10 Mbp non-overlapping segments  
627 from the alignments of the BBO\_3569 (n=123 segments) and BBO\_3574 (n=177 segments)  
628 whole genome sequence onto the UMD 3.1 bovine genome assembly. Time scale was  
629 translated into YBP assuming  $\mu_y = 2.10 \times 10^{-9}$  (Liu, et al. 2006).

630 C. Estimation of the average number of migrant per generation ( $2N_e m$ ) during the divergence  
631 of the BBO and BTA lineages under the Isolation-with-Migration model. The two violin plots

632 show the distribution of the migration rate estimates obtained for each 10 Mbp non-  
633 overlapping segments from the alignments of the BBO\_3569 (n=123 segments) and  
634 BBO\_3574 (n=177 segments) whole genome sequence onto the UMD 3.1 bovine genome  
635 assembly.

636 D. Model comparisons between the isolation and the Isolation-with-Migration models. The  
637 two violin plots show the distribution of the difference between the Akaike Information  
638 Criterion for the isolation ( $AIC_I$ ) and for the isolation-with-migration ( $AIC_{IM}$ ) obtained for  
639 each 10 Mbp non-overlapping segments from the alignments of the BBO\_3569 (n=123  
640 segments) and BBO\_3574 (n=177 segments) whole genome sequence onto the UMD 3.1  
641 bovine genome assembly. Because the model with the smallest  $AIC$  should be preferred, the  
642 distributions provide strong support in favor of the IM-model ( $AIC_{IM}$  is always lower than  
643  $AIC_I$ ).

644

645 **Figure 3. Representation of the genes with a  $Ka/Ks > 1$  connected to their key functions.**

646 Each global function and its links to the corresponding key genes are differently colored i.e. in  
647 purple for nervous system, blue for by-products of domestication, green for functions related  
648 to embryonic, organ development, organismal abnormality and hereditary disorders, pink for  
649 immune and inflammatory responses, orange for reproduction, grey for hair development and  
650 thermogenesis, yellow for lipid metabolism and white for gustation. Global functions contain  
651 genes belonging to several Ingenuity Pathway Analysis functional categories.

652 Gene symbols are colored in red and color intensity is correlated to  $Ka/Ks$  value.

653

## 654 SUPPLEMENTARY TABLE LEGENDS

655 **Table S1: Mapping statistics of the European bison high throughput sequencing reads**  
656 **onto the UMD3.1 bovine reference genome and *OviAr3* ovine reference genome**  
657 **assemblies.**

658

659 **Table S2: Maximum likelihood estimates of the (autosomal) heterozygosities ( $\hat{\theta}$ ) and**  
660 **sequencing error rates ( $\hat{\epsilon}$ ) for the BBO\_3569 and BBO\_3574 individual European bison**  
661 **genomes and the AAN\_0037, JER\_0009, HOL\_0101 and SIM\_0043 individual genomes**  
662 **belonging to the Angus, Jersey, Holstein and Simmental European cattle breeds**  
663 **respectively.** The table also gives the number of sites available in the estimation procedure  
664 (i.e., covered by 10 to 100 read nucleotides after discarding bases with a  $BAQ < 25$ )

665

666 **Table S3: List of the 481 Ensembl transcript ID with a Ka/Ks >1 (from 1.003 to 8.289)**  
667 **mapped in the Ingenuity Pathway Knowledge Base and of their corresponding gene**  
668 **symbol and Entrez gene name. One to one orthologs between cattle and sheep are indicated.**

669 **Table S4: List of the top five significant diseases and biological functions in each main**  
670 **functional categories obtained using Ingenuity Pathway Analysis for the 481 (405)**  
671 **transcripts with a Ka/Ks >1 (one to one orthologs between bovine and sheep).**

672

673 **Table S5: List of the significant functional categories with their corresponding**  
674 **functional annotation, p-value and annotated molecules.**

675

676 **Table S6: List of the significant networks including genes with a Ka/Ks >1, obtained**  
677 **with the Ingenuity Pathway Analysis software.**

678

## 679 **SUPPLEMENTARY FIGURE LEGENDS**

680 **Figure S1: Regional nucleotide divergence between the cattle genome and the BBO\_3569**  
681 **(A) and BBO\_3574 (B) European bison genome sequences over contiguous 10-Mb**  
682 **segments covering the 29 bovine autosomes and the X-chromosome.**

683

684 **Figure S2: Distribution of the heterozygosity estimates across the 29 bovine autosomes**  
685 **based on the BBO\_3569 and BBO\_3574 individual European bison genomes and for the**  
686 **AAN\_0037, JER\_0009, HOL\_0101 and SIM\_0043 individual genomes belonging to the**  
687 **Angus, Jersey, Holstein and Simmental European cattle breeds respectively.**

688

689 **Figure S3: Backward in time (in units of  $2\mu_y T$ ) estimates of the (scaled) effective**  
690 **population sizes (in units of  $4N_e\mu_g$ ) from the analyses of the BBO\_3569 and BBO\_3574**  
691 **individual wisent genomes and the AAN\_0037, HOL\_0101, JER\_0009 and SIM\_0043**  
692 **bull bovine genomes**

693

694 **Figure S4: Bootstrap confidence intervals of the population size histories inferred from**  
695 **the two wisent and the four bovine genomes under the PSMC model. For each**  
696 **individual genome, the dark red curve represents the direct estimation (as in Figure 1A)**

697 **while the 100 orange curves represent estimated history obtained on bootstrap genome**  
698 **samples (Li and Durbin 2011).**

699

700 **Figure S5: Comparison of the population histories inferred by the PSMC algorithm**  
701 **from the two wisent genomes derived by either aligning the underlying sequencing reads**  
702 **onto the UMD 3.1 cattle genome assembly (in black) or the consensus BBO reference**  
703 **assembly (in red).**

704

705 **Figure S6: Distribution of the Ka/Ks estimates obtained for all the BBO/BTA protein**  
706 **sequence alignments.**

707

708 **Figure S7. List of genes with a Ka/Ks ratio>1 participating to the six overlapping**  
709 **significant networks.**

710 Gene symbols are colored in red and color intensity is correlated to Ka/Ks value.

711

## 712 **References**

713

714 Ayub M, Basit S, Jelani M, Ur Rehman F, Iqbal M, Yasinzai M, Ahmad W. 2009. A homozygous  
715 nonsense mutation in the human desmocollin-3 (DSC3) gene underlies hereditary hypotrichosis and  
716 recurrent skin vesicles. *Am J Hum Genet* 85:515-520.

717 Bechtold DA, Sidibe A, Saer BR, Li J, Hand LE, Ivanova EA, Darras VM, Dam J, Jockers R,  
718 Luckman SM, et al. 2012. A role for the melatonin-related receptor GPR50 in leptin signaling,  
719 adaptive thermogenesis, and torpor. *Curr Biol* 22:70-77.

720 Belyaev DK. 1979. The Wilhelmine E. Key 1978 invitational lecture. Destabilizing selection as a  
721 factor in domestication. *J Hered* 70:301-308.

722 Benecke N. 2005. The Holocene distribution of European bison-the archaeozoological record. *Munibe*  
723 *(Antropologia-Arkeologia)* 57:421-428.

724 Bocherens H, Hofman-Kamińska E, Drucker DG, Schmolcke U, Kowalczyk R. 2015. European bison  
725 as a refugee species? Evidence from isotopic data on Early Holocene bison and other large herbivores  
726 in northern Europe. *PLoS One* 10:e0115090.

727 Bradley DG, MacHugh DE, Cunningham P, Loftus RT. 1996. Mitochondrial diversity and the origins  
728 of African and European cattle. *Proc Natl Acad Sci U S A* 93:5131-5135.

729 Buntjer JB, Otsen M, Nijman IJ, Kuiper MT, Lenstra JA. 2002. Phylogeny of bovine species based on  
730 AFLP fingerprinting. *Heredity (Edinb)* 88:46-51.

- 731 Canavez FC, Luche DD, Stothard P, Leite KR, Sousa-Canavez JM, Plastow G, Meidanis J, Souza  
732 MA, Feijao P, Moore SS, et al. 2012. Genome sequence and assembly of *Bos indicus*. *J Hered*  
733 103:342-348.
- 734 Cieslak M, Reissmann M, Hofreiter M, Ludwig A. 2011. Colours of domestication. *Biol Rev Camb*  
735 *Philos Soc* 86:885-899.
- 736 Clark PU, Dyke AS, Shakun JD, Carlson AE, Clark J, Wohlfarth B, Mitrovica JX, Hostetler SW,  
737 McCabe AM. 2009. The Last Glacial Maximum. *Science* 325:710-714.
- 738 Daetwyler HD, Capitan A, Pausch H, Stothard P, van Binsbergen R, Brondum RF, Liao X, Djari A,  
739 Rodriguez SC, Grohs C, et al. 2014. Whole-genome sequencing of 234 bulls facilitates mapping of  
740 monogenic and complex traits in cattle. *Nat Genet* 46:858-865.
- 741 Durand EY, Patterson N, Reich D, Slatkin M. 2011. Testing for ancient admixture between closely  
742 related populations. *Mol Biol Evol* 28:2239-2252.
- 743 Elias SA. 2013. History of Quaternary science. . In: Elias SA, editor. *Encyclopedia of Quaternary*  
744 *Science*, second edition. Amsterdam: Elsevier. p. 10-18.
- 745 Freeman AR, Lynn DJ, Murray C, Bradley DG. 2008. Detecting the effects of selection at the  
746 population level in six bovine immune genes. *BMC Genet* 9:62.
- 747 Gautier M, Faraut T, Moazami-Goudarzi K, Navratil V, Foglio M, Grohs C, Boland A, Garnier JG,  
748 Boichard D, Lathrop GM, et al. 2007. Genetic and haplotypic structure in 14 European and African  
749 cattle breeds. *Genetics* 177:1059-1070.
- 750 Green RE, Krause J, Briggs AW, Maricic T, Stenzel U, Kircher M, Patterson N, Li H, Zhai W, Fritz  
751 MH, et al. 2010. A draft sequence of the Neandertal genome. *Science* 328:710-722.
- 752 Hassanin A, An J, Ropiquet A, Nguyen TT, Couloux A. 2013. Combining multiple autosomal introns  
753 for studying shallow phylogeny and taxonomy of Laurasiatherian mammals: Application to the tribe  
754 Bovini (Cetartiodactyla, Bovidae). *Mol Phylogenet Evol* 66:766-775.
- 755 Haubold B, Pfaffelhuber P, Lynch M. 2010. mlRho - a program for estimating the population mutation  
756 and recombination rates from shotgun-sequenced diploid genomes. *Mol Ecol* 19 Suppl 1:277-284.
- 757 Ho SY, Larson G, Edwards CJ, Heupink TH, Lakin KE, Holland PW, Shapiro B. 2008. Correlating  
758 Bayesian date estimates with climatic events and domestication using a bovine case study. *Biol Lett*  
759 4:370-374.
- 760 Hobolth A, Christensen OF, Mailund T, Schierup MH. 2007. Genomic relationships and speciation  
761 times of human, chimpanzee, and gorilla inferred from a coalescent hidden Markov model. *PLoS*  
762 *Genet* 3:e7.
- 763 Hofreiter M, Stewart J. 2009. Ecological change, range fluctuations and population dynamics during  
764 the Pleistocene. *Curr Biol* 19:R584-594.
- 765 Hurst LD. 2002. The Ka/Ks ratio: diagnosing the form of sequence evolution. *Trends Genet* 18:486.

- 766 Jakob W, Schröder HD, Rudolph M, Krasinski ZA, Krasinska M, Wolf O, Lange A, J.E. C, Frölich K.  
767 2000. Necrobacillosis in free-living male European Bison in Poland. *Journal of Wildlife Diseases*  
768 36:248-256.
- 769 Jiang Y, Xie M, Chen W, Talbot R, Maddox JF, Faraut T, Wu C, Muzny DM, Li Y, Zhang W, et al.  
770 2014. The sheep genome illuminates biology of the rumen and lipid metabolism. *Science* 344:1168-  
771 1173.
- 772 Keightley PD, Eyre-Walker A. 2000. Deleterious mutations and the evolution of sex. *Science* 290:331-  
773 333.
- 774 Kent WJ. 2002. BLAT--the BLAST-like alignment tool. *Genome Res* 12:656-664.
- 775 Kerley GIH, Kowalczyk R, Cromsigt PGM. 2012. Conservation implications of the refugee species  
776 concept and the European bison: king of the forest or refugee in a marginal habitat? *Ecography*  
777 35:519-529.
- 778 Kimura M. 1983. The neutral theory of molecular evolution. Cambridge: Cambridge University Press.
- 779 Kowalczyk R, Taberlet P, Coissac E, Valentini A, Miquel C, Kamiński T, Wojcik JM. 2011. Influence  
780 of management practices on large herbivore diet-Case of European bison in Białowieża Primeval  
781 Forest (Poland). *Forest Ecology and Management* 261:821-828.
- 782 Krasinska M, Krasinski ZA. 2002. Body mass and measurements of the European bison during  
783 postnatal development. *Acta Theriologica* 47:85-106.
- 784 Kuemmerle T, Hickler T, Olofsson J, Schurgers G, Radeloff V. 2012. Reconstructing range dynamics  
785 and range fragmentation of European bison for the last 8000 years. *Diversity and Distributions* 18:47-  
786 59.
- 787 Li H, Durbin R. 2009. Fast and accurate short read alignment with Burrows-Wheeler transform.  
788 *Bioinformatics* 25:1754-1760.
- 789 Li H, Durbin R. 2011. Inference of human population history from individual whole-genome  
790 sequences. *Nature* 475:493-496.
- 791 Li WH, Yi S, Makova K. 2002. Male-driven evolution. *Curr Opin Genet Dev* 12:650-656.
- 792 Lister AM, A.J. S. 2008. The impact of climate change on large mammal distribution and extinction:  
793 Evidence from the last glacial/interglacial transition. *C.R. Geoscience* 340:615-620.
- 794 Liu GE, Matukumalli LK, Sonstegard TS, Shade LL, Van Tassell CP. 2006. Genomic divergences  
795 among cattle, dog and human estimated from large-scale alignments of genomic sequences. *BMC*  
796 *Genomics* 7:140.
- 797 Liu Y, Qin X, Song XZ, Jiang H, Shen Y, Durbin KJ, Lien S, Kent MP, Sodeland M, Ren Y, et al.  
798 2009. Bos taurus genome assembly. *BMC Genomics* 10:180.
- 799 Lorenzen ED, Noguez-Bravo D, Orlando L, Weinstock J, Binladen J, Marske KA, Ugan A,  
800 Borregaard MK, Gilbert MT, Nielsen R, et al. 2011. Species-specific responses of Late Quaternary  
801 megafauna to climate and humans. *Nature* 479:359-364.

- 802 Lynch M. 2008. Estimation of nucleotide diversity, disequilibrium coefficients, and mutation rates  
803 from high-coverage genome-sequencing projects. *Mol Biol Evol* 25:2409-2419.
- 804 Macleod IM, Larkin DM, Lewin HA, Hayes BJ, Goddard ME. 2013. Inferring demography from runs  
805 of homozygosity in whole-genome sequence, with correction for sequence errors. *Mol Biol Evol*  
806 30:2209-2223.
- 807 Mailund T, Dutheil JY, Hobolth A, Lunter G, Schierup MH. 2011. Estimating divergence time and  
808 ancestral effective population size of Bornean and Sumatran orangutan subspecies using a coalescent  
809 hidden Markov model. *PLoS Genet* 7:e1001319.
- 810 Mailund T, Halager AE, Westergaard M, Dutheil JY, Munch K, Andersen LN, Lunter G, Prufer K,  
811 Scally A, Hobolth A, et al. 2012. A new isolation with migration model along complete genomes  
812 infers very different divergence processes among closely related great ape species. *PLoS Genet*  
813 8:e1003125.
- 814 Mazet O, Rodriguez W, Grusea S, Boitard S, Chikhi L. 2015. On the importance of being structured:  
815 instantaneous coalescence rates and human evolution-lessons for ancestral population size inference?  
816 *Heredity (Edinb)*.
- 817 Merceron G, Hofman-Kamińska E, Kowalczyk R. 2014. 3D dental microwear texture analysis of  
818 feeding habits of sympatric ruminants in the Białowieża Primeval Forest, Poland. *Forest Ecology and*  
819 *Management* 328:262-269.
- 820 Mikkelsen TS, Hillier LH, Eichler EE, Zody MC, Jaffe DB, Yang SP, Enard W, Hellmann I,  
821 Lindblad-Toh K, Altheide TK, et al. 2005. Initial sequence of the chimpanzee genome and comparison  
822 with the human genome. *Nature* 437:69-87.
- 823 Mona S, Catalano G, Lari M, Larson G, Boscato P, Casoli A, Sineo L, Di Patti C, Pecchioli E,  
824 Caramelli D, et al. 2010. Population dynamic of the extinct European aurochs: genetic evidence of a  
825 north-south differentiation pattern and no evidence of post-glacial expansion. *BMC Evol Biol* 10:83.
- 826 Nevado B, Ramos-Onsins SE, Perez-Enciso M. 2014. Resequencing studies of nonmodel organisms  
827 using closely related reference genomes: optimal experimental designs and bioinformatics approaches  
828 for population genomics. *Mol Ecol* 23:1764-1779.
- 829 Penck A, Brückner E. 1901-1909. Die Alpen im Eiszeitalter. Leipzig: Tauchnitz.
- 830 Pucek Z. 2004. European Bison. In: Pucek Z, Belousova Z, Krasieńska M, Krasieński ZA, Olech W,  
831 Group ISBS, editors. Status Survey and Conservation Action Plan. Gland, Switzerland and  
832 Cambridge, UK: IUCN-The World Conservation Union. p. 54.
- 833 Raczynski J. 2015. European bison pedigree book 2014: Białowieża National Park.
- 834 Reissmann M, Ludwig A. 2013. Pleiotropic effects of coat colour-associated mutations in humans,  
835 mice and other mammals. *Semin Cell Dev Biol* 24:576-586.
- 836 Shapiro B, Drummond AJ, Rambaut A, Wilson MC, Matheus PE, Sher AV, Pybus OG, Gilbert MT,  
837 Barnes I, Binladen J, et al. 2004. Rise and fall of the Beringian steppe bison. *Science* 306:1561-1565.

- 838 Shimomura Y, Wajid M, Petukhova L, Kurban M, Christiano AM. 2010. Autosomal-dominant woolly  
839 hair resulting from disruption of keratin 74 (KRT74), a potential determinant of human hair texture.  
840 *Am J Hum Genet* 86:632-638.
- 841 Soares P, Achilli A, Semino O, Davies W, Macaulay V, Bandelt HJ, Torroni A, Richards MB. 2010.  
842 The archaeogenetics of Europe. *Curr Biol* 20:R174-183.
- 843 Sommer RS, Nadachowski A. 2006. Glacial refugia of mammals in Europe:evidence from fossil  
844 records. *Mammal rev.* 36:251-265.
- 845 Tokarska M, Marshall T, Kowalczyk R, Wojcik JM, Pertoldi C, Kristensen TN, Loeschcke V,  
846 Gregersen VR, Bendixen C. 2009. Effectiveness of microsatellite and SNP markers for parentage and  
847 identity analysis in species with low genetic diversity: the case of European bison. *Heredity (Edinb)*  
848 103:326-332.
- 849 Tokarska M, Pertoldi C, Kowalczyk R, Perzanowski K. 2011. Genetic status of the European bison  
850 *Bison bonasus* after extinction in the wild and subsequent recovery. *Mammal Review* 41:151-162.
- 851 Troy CS, MacHugh DE, Bailey JF, Magee DA, Loftus RT, Cunningham P, Chamberlain AT, Sykes  
852 BC, Bradley DG. 2001. Genetic evidence for Near-Eastern origins of European cattle. *Nature*  
853 410:1088-1091.
- 854 Trut L, Oskina I, Kharlamova A. 2009. Animal evolution during domestication: the domesticated fox  
855 as a model. *Bioessays* 31:349-360.
- 856 Verkaar EL, Nijman IJ, Beeke M, Hanekamp E, Lenstra JA. 2004. Maternal and paternal lineages in  
857 cross-breeding bovine species. Has wisent a hybrid origin? *Mol Biol Evol* 21:1165-1170.
- 858 Wilkins AS, Wrangham RW, Fitch WT. 2014. The "domestication syndrome" in mammals: a unified  
859 explanation based on neural crest cell behavior and genetics. *Genetics* 197:795-808.
- 860 Wójcik JM, Kawałko A, Tokarska M, Jaarola M, Vallenback P, Pertoldi C. 2009. Post-bottleneck  
861 mtDNA diversity in a free-living population of European bison: implication for conservation. *Journal*  
862 *of Zoology* 277:81-87.
- 863 Zhang Z, Li J, Zhao XQ, Wang J, Wong GK, Yu J. 2006. KaKs\_Calculator: calculating Ka and Ks  
864 through model selection and model averaging. *Genomics Proteomics Bioinformatics* 4:259-263.

865

866

## 867 **FIGURES**

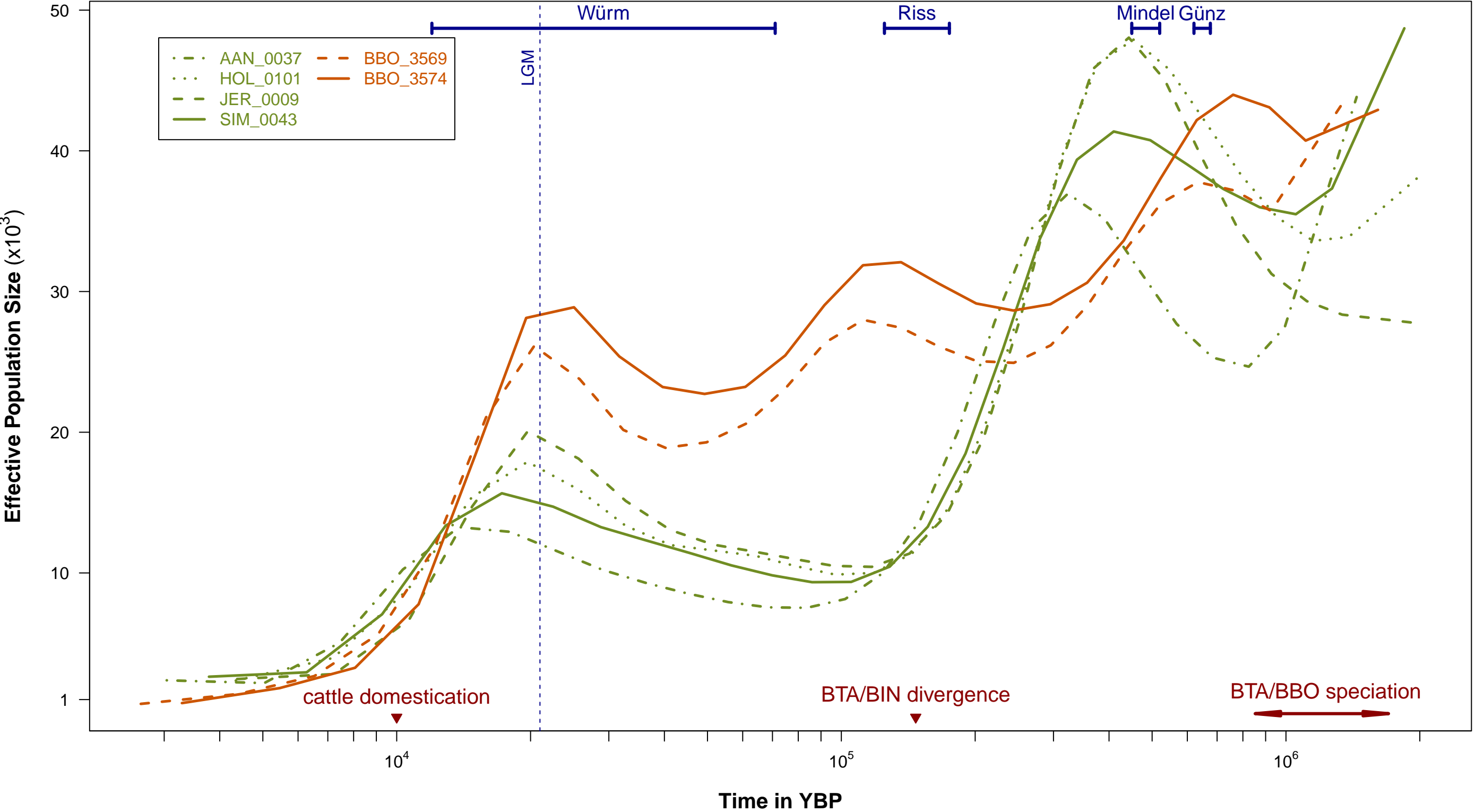
868

869 **Figure 1**

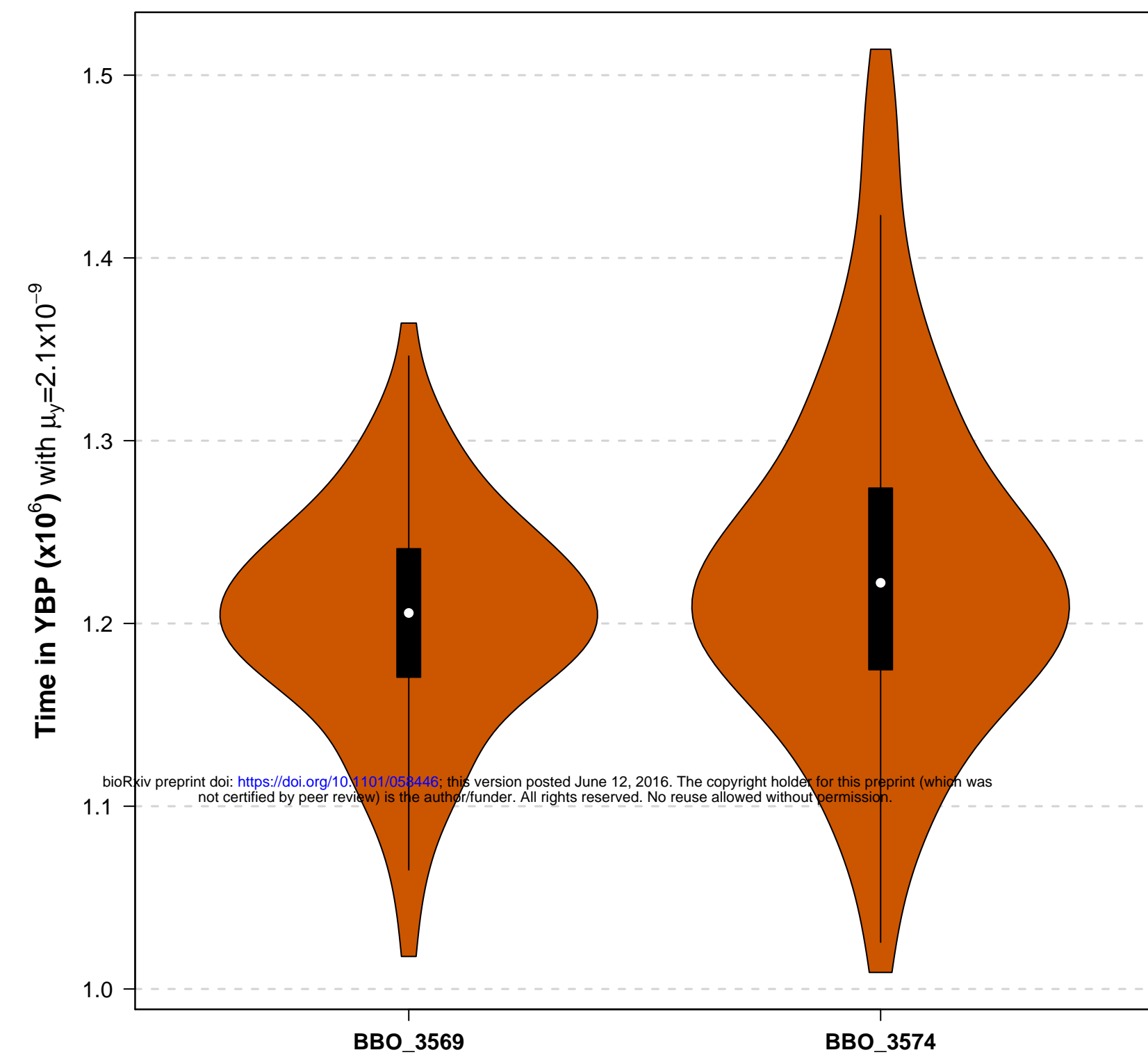
870 **Figure 2**

871 **Figure 3**

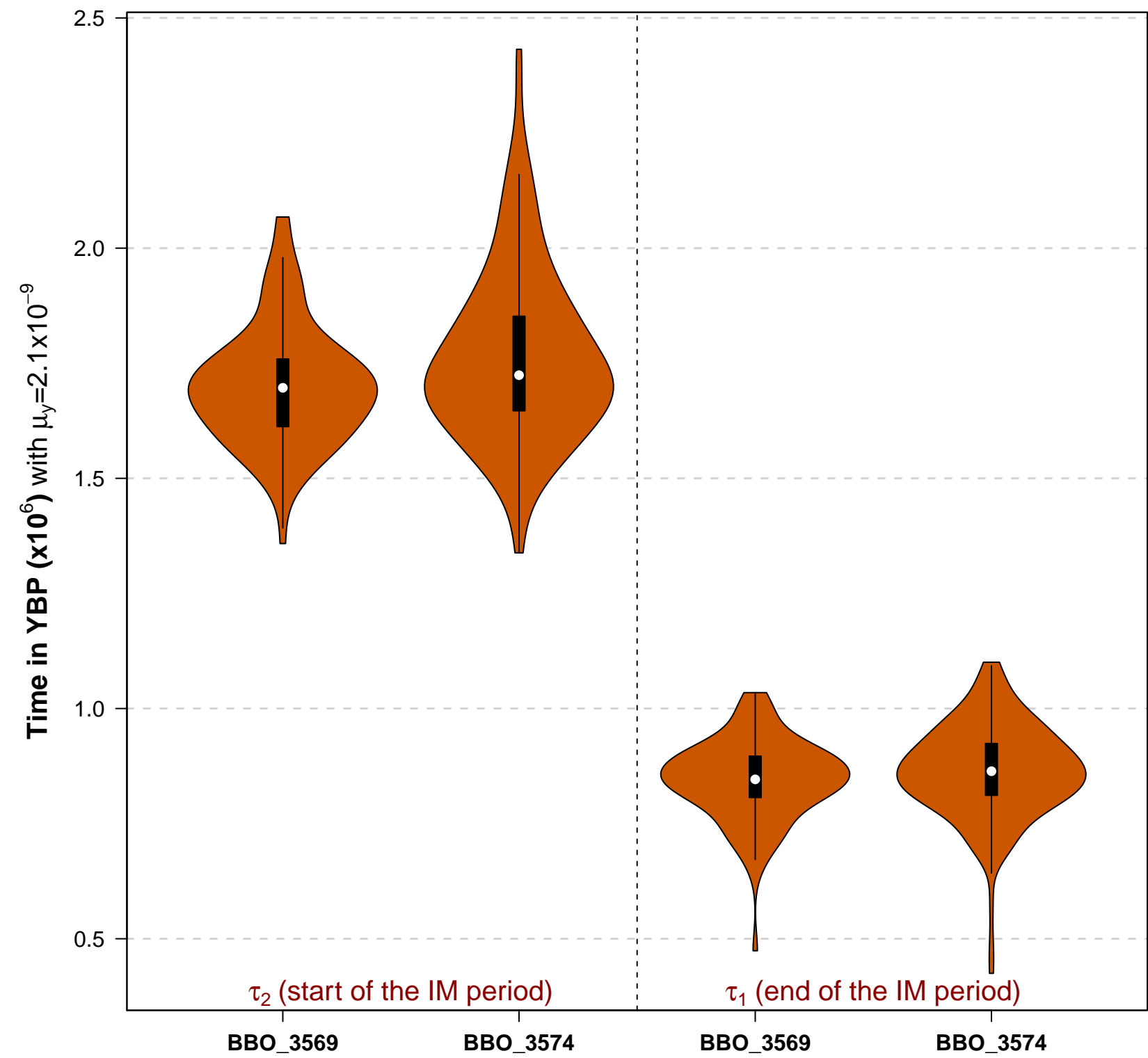
Population Size History in real units (assuming  $\mu_y = 2.1 \times 10^{-9}$  and  $g=6$ )



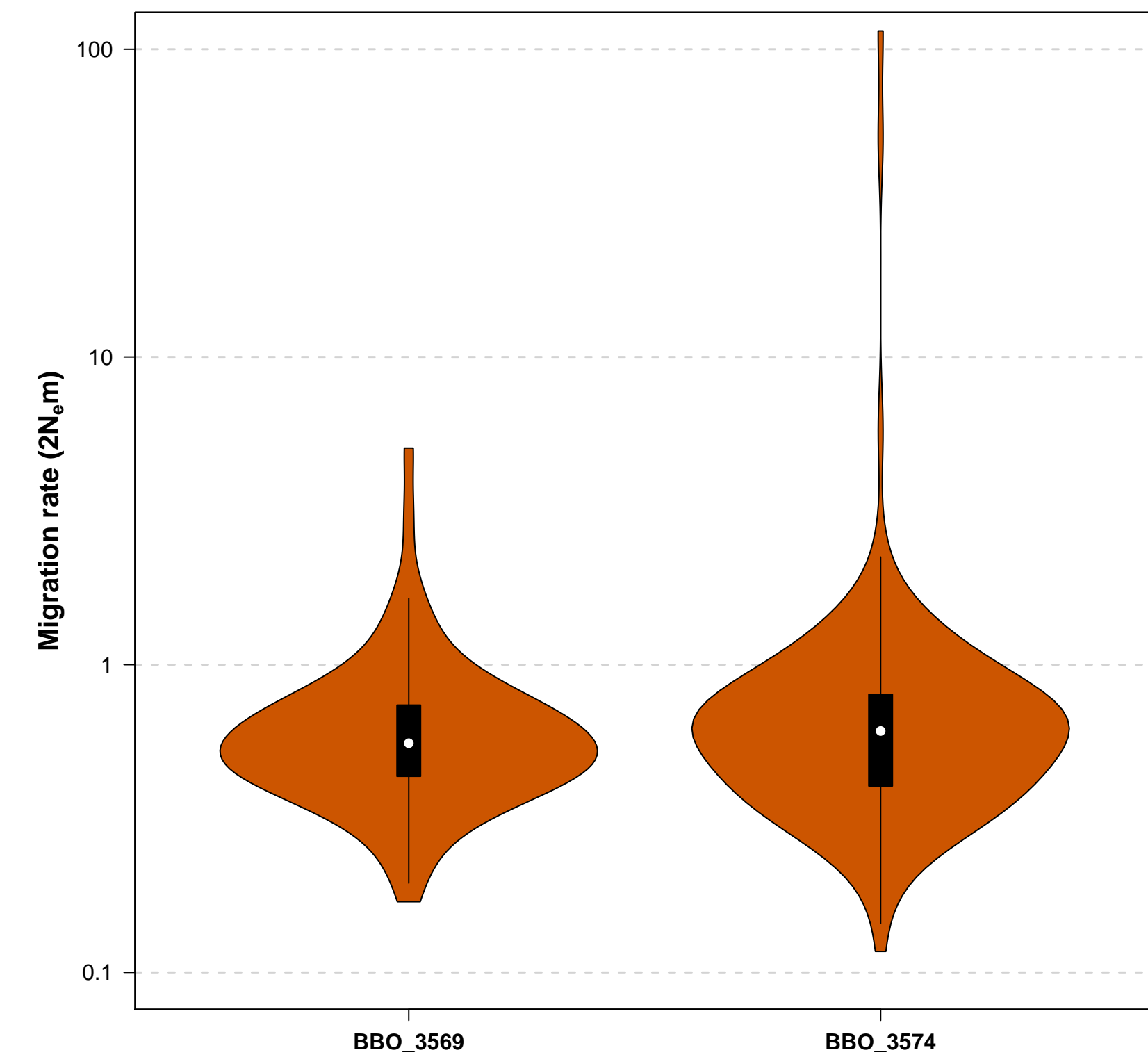
**A) Estimates of  $\tau_D$  under the I-model**



**B) Estimates of  $\tau_1$  and  $\tau_2$  under the IM-model**



**C) Estimates of the migration rate under the IM-model**



**D) AIC-based comparison of the I and IM models**

